

# The emission-line spectrum of KUG 1031+398 and the Intermediate Line Region <sup>\*</sup>

A. C. Gonçalves, P. Véron, and M.-P. Véron-Cetty

Observatoire de Haute-Provence (CNRS), F-04870 Saint Michel l'Observatoire, France

Received / Accepted

**Abstract.** We present results based on the analysis of optical spectra of KUG 1031+398, a Narrow Line Seyfert 1 (NLS1) galaxy for which Mason et al. (1996) reported evidence for a line-emitting region “intermediate” (both in terms of velocity and density) between the conventional broad and narrow line regions (BLR and NLR, respectively). From our observations and modelling of the spectra, we get a consistent decomposition of the line profiles into four components: an extended H II region with unresolved lines, two distinct Seyfert-type clouds identified with the NLR, and a relatively narrow “broad line” component emitting only Balmer lines but no forbidden lines. Therefore, and although we find this object to be exceptional in having line-emission from the BLR with almost the same width as the narrow lines, our interpretation of the data does not support the existence of an “intermediate” line region (ILR).

**Key words:** galaxies: active – galaxies: Seyfert – galaxies: individual: KUG 1031+398

## 1. Introduction

### 1.1. The Intermediate Line Region

It is commonly accepted that line-emission in AGNs comes from two well separated regions: one, compact (smaller than 1 pc) and lying close to the central engine, has a high electron density ( $N_e > 10^8 \text{ cm}^{-3}$ ) and is responsible for the production of broad (FWHM  $\sim$  thousands of  $\text{km s}^{-1}$ ) permitted lines – the BLR; the other, more extended and lying further away from the central source (10–1 000 pc), has lower electron densities ( $10^3 \leq N_e \leq 10^5 \text{ cm}^{-3}$ ) and emits lines with a lower velocity dispersion ( $\sim$  hundreds of  $\text{km s}^{-1}$ ) – the NLR.

A line-emission “gap” is usually observed between the two regions, most objects showing an optical spectrum which can be fitted by line profiles corresponding to clouds belonging to one or the other line-emitting regions. This line-emission gap can be explained by the presence of dust mixed with the gas (Netzer & Laor 1993). Nevertheless, the existence of an inter-

mediate region, both in terms of velocity and density, is expected; in such a region, the [O III] lines would be partially collisionally de-excited<sup>1</sup> and show substantially broadened wings (Shields 1978). This ILR should not be confused with the ILR found in QSOs by Brotherton et al. (1994), which is much smaller and denser, with a velocity dispersion of the order of  $2\,000 \text{ km s}^{-1}$  and density  $\sim 10^{10} \text{ cm}^{-3}$ .

Mason et al. (1996) presented high-resolution ( $2 \text{ \AA}$ ) optical spectroscopic observations of KUG 1031+398. The model they used to fit the data revealed a line-emitting region with lines of intermediate width (FWHM  $\sim 1\,000 \text{ km s}^{-1}$ ); according to Mason et al., this region would dominate the Balmer lines profile, being also a significant contributor to the [O III] $\lambda\lambda 4959, 5007$  lines, with a flux ratio  $\lambda 5007/\text{H}\beta = 1.4$ , suggesting an intermediate density.

Osterbrock (1978) thought that he had detected, in a few Seyfert 1 galaxies, faint wings to the [O III] lines with essentially the same widths as the Balmer lines. Crenshaw & Peterson (1986) and van Groningen & de Bruyn (1989) have found broad wings in the [O III] lines of a number of Seyfert 1 galaxies, implying the presence, in these objects, of an ILR with a density of a few times  $10^6 \text{ cm}^{-3}$ , similar to the one reported in KUG 1031+398; however, all these objects show strong Fe II emission, and the observed broad [O III] components could be due to an inaccurate removal of the Fe II blends (Boroson & Green 1992).

In summary, although the presence in Seyfert 1 galaxies of emitting clouds with density intermediate between those of the “broad” and “narrow” components is not unexpected, no uncontroversial report of the existence of such intermediate components has ever been made to the best of our knowledge. Therefore, the claims by Mason et al. (1996) that the NLS1 KUG 1031+398 shows evidence for an ILR induced us to conduct new spectroscopic observations and modelling of its emission-line features.

<sup>1</sup> If we make the assumptions that the excitation conditions in both the NLR and the ILR are the same and that in the ILR,  $\lambda 5007/\text{H}\beta \sim 1$ , the [O III] $\lambda 5007$  line is collisionally de-excited by about a factor 10. According to the formula given by Seaton (1975), this implies a density of  $1\text{--}3 \cdot 10^6 \text{ cm}^{-3}$  if the electronic temperature is in the range  $1\text{--}3 \cdot 10^4 \text{ K}$ .

Send offprint requests to: A. C. Gonçalves, anabela@obs-hp.fr

<sup>\*</sup> Based on observations collected at the Observatoire de Haute-Provence (CNRS), France.

## 1.2. KUG 1031+398

2RE J1034+396 was found in the *ROSAT* Wide Field Camera all-sky extreme-ultraviolet survey (Pounds et al. 1993; Pye et al. 1995). It was identified by Shara et al. (1993) and Mason et al. (1995) with the compact UV-excess 15.0 mag galaxy KUG 1031+398 (Takase & Miyauchi-Isobe 1987) at  $z = 0.042$ . This object has an intense soft X-ray emission with an unusually steep 2–10 keV power law of photon index  $\Gamma \sim 2.6 \pm 0.1$  (Pounds et al. 1995) and an even steeper 0.1–2.4 keV power law with  $\Gamma = 3.4 \pm 0.3$  (Puchnarewicz et al. 1995) or  $\Gamma = 4.4 \pm 0.1$  (Rodríguez-Pascual et al. 1997).

UV spectroscopy with the *Hubble Space Telescope* shows the Ly $\alpha$  profile to be complex, with a narrow (400 km s<sup>-1</sup> FWHM) and a broad (1600 km s<sup>-1</sup> FWHM) component (Puchnarewicz et al. 1998). The optical continuum is not polarized (Breeveld & Puchnarewicz 1998).

The broad component of the Balmer lines is relatively narrow (FWHM  $\sim 1500$  km s<sup>-1</sup>) and, consequently, this object has been classified as a NLS1 by Puchnarewicz et al. (1995). Narrow line Seyfert 1 galaxies are defined as Seyfert 1s having “broad” Balmer lines narrower than 2000 km s<sup>-1</sup> FWHM (Osterbrock 1987). Most NLS1s have a steep soft ( $< 1$  keV) X-ray component and, conversely, most ultra-soft X-ray sources are associated with a NLS1 (Puchnarewicz et al. 1992; Greiner et al. 1996; Boller et al. 1996; Wang et al. 1996).

## 2. Observations

Spectroscopic observations of KUG 1031+398 were carried out with the spectrograph CARELEC (Lemaître et al. 1989) attached to the Cassegrain focus of the Observatoire de Haute Provence (OHP) 1.93 m telescope. The detector was a 512×512 pixels, 27×27  $\mu\text{m}$  Tektronix CCD. We used a 600 l mm<sup>-1</sup> grating giving a dispersion of 66 Å mm<sup>-1</sup>. On January 10, 1997 we obtained a 20 min exposure in the range  $\lambda\lambda$  6175–7075 Å, on March 4, a 20 min exposure in the range  $\lambda\lambda$  4780–5780 Å, and three more on March 5.

The slit width was 2''1, corresponding to a projected slit width on the detector of 52  $\mu\text{m}$ , or 1.9 pixel. The resolution, as measured on the night sky emission lines, was 3.4 Å FWHM in the blue and 3.5 Å in the red. In both cases the galaxy nucleus was centered on the slit and 3 columns of the CCD ( $\sim 3''2$ ) were extracted, corresponding to  $\sim 4$  kpc at the distance of the galaxy (with  $H_0 = 50$  km s<sup>-1</sup> Mpc<sup>-1</sup>).

The spectra were flux calibrated using the standard stars EG 247 (Oke 1974) and Feige 66 (Massey et al. 1988), observed with the same instrumental settings; these standards were also used to correct the red spectrum for the atmospheric B band at  $\lambda 6867$  Å (Fig. 1b).

## 3. Analysis

### 3.1. Methodology

Positive correlations between line-widths and ionization potentials/critical densities have been observed in the narrow line re-

gion of many Seyfert galaxies. Negative correlations are also sometimes found. A positive correlation implies that the density and/or ionization parameter gradually increases inward in the NLR of these objects. In the case of correlations with critical densities, the observed values range from  $\sim 10^3$  to  $\sim 3 \cdot 10^6$  cm<sup>-3</sup> (Filippenko & Sargent 1985).

Sub-structures were found in the narrow line profiles of most objects suggesting that the line emitting region is a collection of individual clouds in motion relative to each other and producing different parts of the line profiles (see for instance Veilleux 1991, Espey et al. 1994 or Ferguson et al. 1997).

These findings induced us to assume that each of these clouds is characterized by a single density and that lines coming from the same emission-region should have the same profile and mean velocity. We therefore tried to model the spectra of KUG 1031+398 with the smallest possible number of line sets, each set including three Gaussians (modelling H $\alpha$  and the [N II] $\lambda\lambda$ 6548, 6583 lines, or H $\beta$  and the [O III] $\lambda\lambda$ 4959, 5007 lines) having the same velocity shift and width, with the additional constraint that the intensity ratio of the two [N II] (respectively [O III]) lines was taken to be equal to the theoretical value of 3.00 (respectively 2.96) (Osterbrock 1974). In a physically meaningful and self-consistent model, the components found when fitting the blue and red spectra should have velocity shifts and widths compatible within the measurement errors.

### 3.2. The narrow line-core components

The spectra were deredshifted assuming  $z = 0.0434$  (Fig. 1a and b) and analysed in terms of Gaussian components as described above. We discovered first that the core of the lines could not be fitted by a single set of narrow Gaussian profiles. To get a satisfactory fit, two sets of Gaussian components are needed: the first, unresolved (and subsequently taken as the origin of the velocity scales) has  $\lambda 6583/\text{H}\alpha = 0.55$  and  $\lambda 5007/\text{H}\beta = 1.27$  and corresponds to a H II region (Fig. 2); the second is resolved (FWHM  $\sim 350$  km s<sup>-1</sup>, corrected for the instrumental broadening), blueshifted by  $\sim 95$  km s<sup>-1</sup> with respect to the narrower components and has line intensity ratios typical of a Seyfert 2 ( $\lambda 6583/\text{H}\alpha = 0.84$ ,  $\lambda 5007/\text{H}\beta = 10.2$ ).

### 3.3. The “broad” components

At this stage, we removed from the blue and red spectra the best fitting line-core (the H II region and the Seyfert 2 nebulousity, Fig. 1c and d), obtaining two spectra we shall call “original data minus core”. The blue one was then fitted with a broad H $\beta$  Gaussian component and two sets of three components modelling the narrow H $\beta$  and [O III] $\lambda\lambda$ 4959, 5007 lines. The result is very suggestive: one set has a strong H $\beta$  line and very weak negative [O III] components, while the other set displays a strong [O III] contribution and a weak negative H $\beta$  component, showing that we have in fact a H $\beta$  component with no associated [O III] emission and [O III] lines with a very weak (undetected) associated H $\beta$ ; in other words, the region produc-

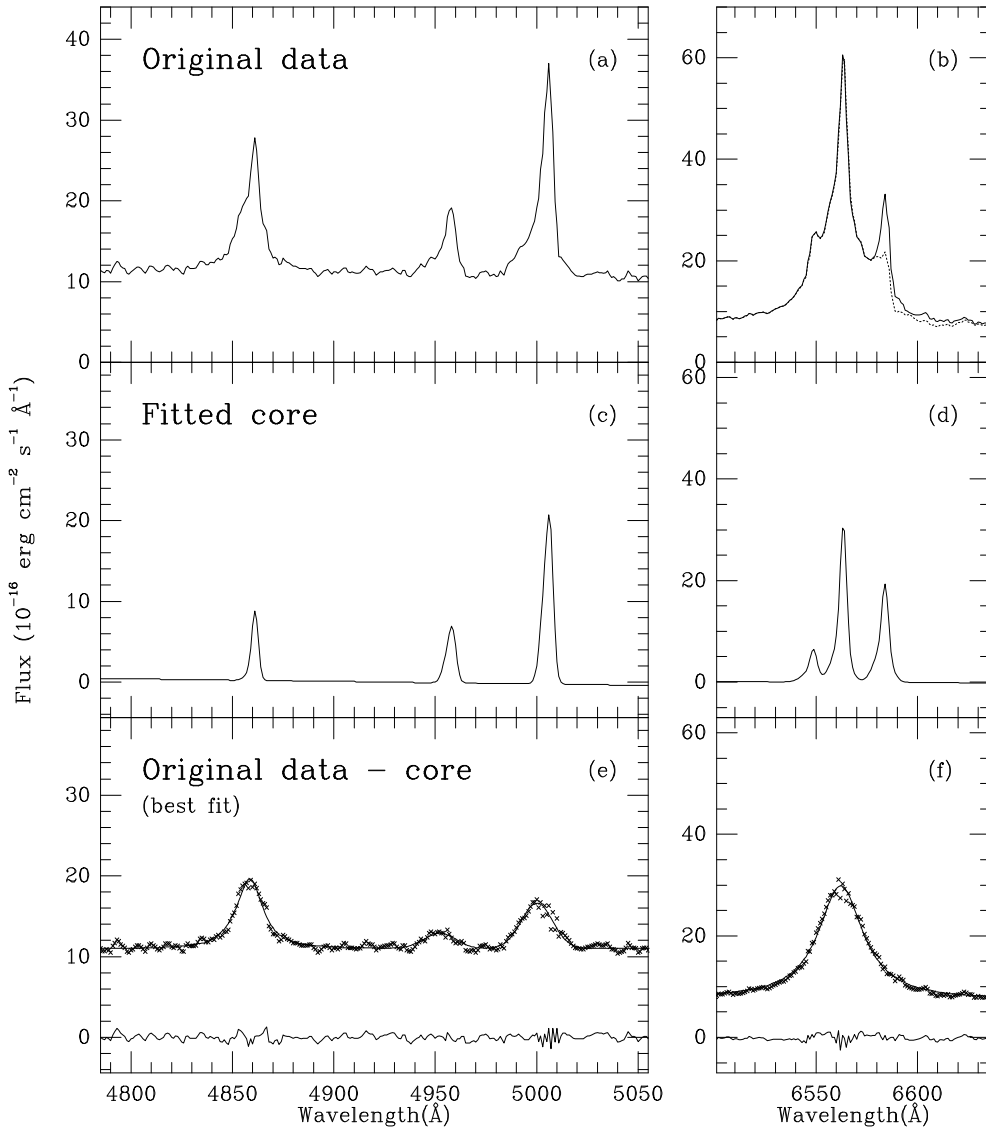


**Fig. 1.** Blue (a) and red (b) spectra of KUG 1031+398 in the rest frame; in (b) we also give the spectrum before correcting for the atmospheric absorption (dotted line). The narrow line-core components (c and d) were fitted with Gaussians and subtracted from the original data, the result being shown in (e) to (h). In (e) and (f), we show our best fit (solid line) together with the data points (crosses); the lower solid lines represent the residuals.

ing the  $H\beta$  line does not emit forbidden lines, while the [O III] emitting region has a high  $\lambda 5007/H\beta$  ratio, which are, respectively, the characteristics of the “broad” and “narrow” line regions in Seyfert 1 galaxies.

Having these results in mind, we optimized this last fit by using a Lorentzian profile for the  $H\beta$  line, with no associated [O III] emission, and a set of three Gaussians for the remaining contribution coming from the “narrow” components (this is not the first time Lorentzian profiles are used to fit AGN emission lines; for example Stüwe et al. (1992) found that, in the case of NGC 4258, the narrow lines were better fitted by Lorentzians, rather than Gaussians).

The best fit is presented in Fig. 1e: in this model, the flux of the “narrow” (Gaussian)  $H\beta$  component is only 9% of the “broad” (Lorentzian)  $H\beta$  component. The  $H\beta$  Lorentzian component is blueshifted by  $150 \text{ km s}^{-1}$  with a width of  $915 \text{ km s}^{-1}$ . The Gaussian components are blueshifted by  $\sim 395 \text{ km s}^{-1}$  and their width is  $\sim 1115 \text{ km s}^{-1}$ . Mason et al. found a FWHM =  $1030 \pm 150 \text{ km s}^{-1}$  for this component which is

blueshifted by  $240 \pm 30 \text{ km s}^{-1}$ . This blueshift, however, is measured with respect to the [O III] lines core which is dominated by the Seyfert 2 cloud, itself blueshifted by  $95 \text{ km s}^{-1}$  with respect to the H II region; the blueshift of Mason et al.’s intermediate component is, therefore,  $240 + 95 = 335 \text{ km s}^{-1}$ , in agreement with our value of  $395 \text{ km s}^{-1}$ .

In Seyfert 1 galaxies, the Balmer decrement of the broad component is never smaller than that of the narrow component; in the present case, we therefore expect the “narrow”  $H\alpha$  component flux to be less than 9% of the “broad”  $H\alpha$  component flux. Moreover, the [N II] $\lambda 6583$  line flux is, in Seyfert galaxies, equal or smaller than the narrow  $H\alpha$  component flux. So, in KUG 1031+398, we expect the narrow lines to be quite weak compared to the “broad”  $H\alpha$  component, and we fitted the “original data minus core” red spectrum with a single Lorentzian profile of  $1205 \text{ km s}^{-1}$  FWHM, blueshifted by  $65 \text{ km s}^{-1}$  with respect to the H II region. This fit is shown in Fig. 1f.

Another model allowing, in addition, for a set of  $H\alpha$  and [N II] Gaussian components was also tested, resulting in a fit

of similar quality; the very small  $\lambda 6583/\text{H}\alpha$  ratio observed for this solution (0.2), shows that the nitrogen lines may be considered as undetectable.

#### 4. Results and Discussion

Our new observations and modelling of KUG 1031+398 yield a consistent decomposition of the emission-line profile into four components (see Table 1):

1. An extended H II region with unresolved lines (Fig. 2);
2. A first Seyfert-type cloud with relatively narrow lines ( $\sim 350 \text{ km s}^{-1}$  FWHM), blueshifted by  $95 \text{ km s}^{-1}$ , belonging to the NLR;
3. A second Seyfert-type component with somewhat broader lines, blueshifted by  $\sim 395 \text{ km s}^{-1}$ ; the width of the lines in this component ( $\sim 1115 \text{ km s}^{-1}$  FWHM), which may seem large for a Seyfert 2, is not exceptional as the FWHM of the lines in the prototype Seyfert 2 galaxy NGC 1068 is  $\sim 1670 \text{ km s}^{-1}$  (Alloin et al. 1983). Only the [O III] lines are observed in this component, with  $\lambda 5007/\text{H}\beta \sim 6.1$ , a line ratio characteristic of NLRs;
4. Finally, a Narrow Line Seyfert 1 cloud with lines well fitted by a Lorentzian profile of  $\sim 1060 \text{ km s}^{-1}$  FWHM, blueshifted by  $105 \text{ km s}^{-1}$ .

Our analysis shows that the emission line spectrum of KUG 1031+398 can be satisfactorily decomposed in a set of components which have line ratios characteristics of H II regions or conventional NLR or BLR clouds, without the need to invoke the presence of an ILR characterized by  $\lambda 5007/\text{H}\beta \sim 1$ .

There are two main reasons why our analysis yields different results from those published by Mason et al. (1996). First, KUG 1031+398 having a redshift of  $\sim 0.043$ , the [N II] $\lambda$  6583 line coincides with the atmospheric B band. When correcting for this absorption feature, the [N II] true intensity is recovered (Fig. 1b) and our red spectrum appears different from the published one; different line-ratios and widths are therefore not unexpected.

Second, the line-profile analysis of Mason et al. differs from ours in that, while we force each Balmer component to be associated with forbidden lines having the same velocity and width, Mason et al. allow these parameters to have different values for the Balmer and forbidden line components. As a result, they found three  $\text{H}\beta$  components (a narrow, an intermediate and a broad one), as well as two [O III] components (a narrow and an intermediate one); they also detected three  $\text{H}\alpha$  components (again a narrow, an intermediate and a broad one), but only a single [N II] component (narrow). The measured width of the narrow  $\text{H}\beta$  component is  $150 \pm 20 \text{ km s}^{-1}$  FWHM, while the width of the narrow [O III] lines is  $265 \pm 10 \text{ km s}^{-1}$ ; this last value, significantly larger than the narrow  $\text{H}\beta$  line width, suggests that the [O III] lines may have a complex profile. Moreover, the width of the [N II] lines is found to be significantly larger ( $400 \pm 60 \text{ km s}^{-1}$ ) than that of the narrow  $\text{H}\alpha$  component ( $190 \pm 40 \text{ km s}^{-1}$ ); this could be due to an in-

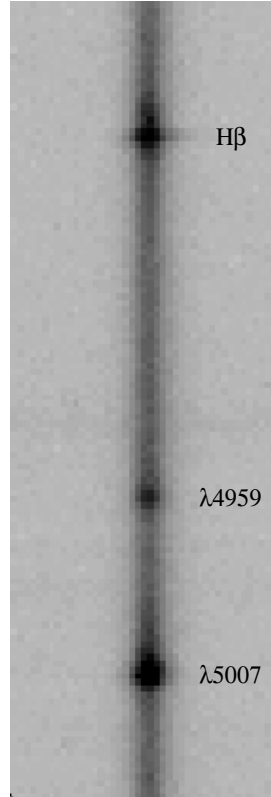


**Fig. 2.** Enlargement of part of the CCD frame showing the  $\text{H}\beta$  and [O III] $\lambda\lambda$ 4959, 5007 lines in the spectrum of KUG 1031+398 (average of three 20 min exposures, after cosmic rays removal); the extended (narrow) component of  $\text{H}\beta$  is clearly visible.

accurate correction of the atmospheric B band, as we have seen above.

Although our spectra have a lower resolution than those obtained by Mason et al. ( $3.4 \text{ \AA}$  compared to  $2 \text{ \AA}$  FWHM), this does not affect the analysis; the narrow core components being identified and subtracted, all the discussion is centered on the broader components, well resolved even with our lower resolution. Similarly, the larger slit width used in our observations ( $2''1$  compared to  $1''5$  for Mason et al.) does not affect the study of these broader components, since only the contribution from the extended emitting region (the H II region, Fig. 2), removed with the core, changes with the slit width.

Boller et al. (1996) and Wang et al. (1996) have suggested that the small width of the broad Balmer lines and the soft X-ray excess characteristic of NLS1 galaxies could be the effect of a high accretion rate on an abnormally small mass black hole. Mason et al. (1996) have argued that, although the emission line spectrum in KUG 1031+398 is dominated by the ILR, a weak broad component is present with line-widths of the order of  $2500 \text{ km s}^{-1}$  FWHM and that, therefore, at least in this object, such a model is not required.

Our analysis of the spectra of KUG 1031+398 has shown that, in the BLR, the Balmer lines are well fitted by a Lorentzian profile with  $\sim 1060 \text{ km s}^{-1}$  FWHM; this value is much narrower than the value found by Mason et al. ( $\sim 2500 \text{ km s}^{-1}$ ). This is due to the fact that we used a Lorentzian, rather than a Gaussian profile to fit the broad Balmer lines; the Lorentzian profile was required by the presence of broad wings, fitted with a Gaussian by Mason et al. (1996).

We have shown (Gonçalves et al. in preparation) that in NLS1s the broad component of the Balmer lines is generally better fitted by a Lorentzian than by a Gaussian; the Lorentzian Balmer lines (component 4), without any measurable associated forbidden line, would qualify this object as a NLS1 with, in fact, very narrow lines. So, in this respect, KUG 1031+398 is a normal NLS1 and could be explained by the same small black hole mass model as the other objects of this class.

**Table 1.** Emission line profile analysis of KUG 1031+398.  $I(H\beta)$  and  $I(H\alpha)$  are in units of  $10^{-16}$  erg s $^{-1}$  cm $^{-2}$ . In columns 1 and 2 we give the mean of the relative velocities and widths measured on the blue and red spectra. The FWHMs are corrected for the instrumental broadening.

	$\Delta V$ (km s $^{-1}$ )	FWHM (km s $^{-1}$ )	$\frac{\lambda 5007}{H\beta}$	$\frac{\lambda 6583}{H\alpha}$	$I(H\beta)$	$I(H\alpha)$
1	0	<80	1.27	0.55	29	93
2	-95	350	10.2	0.84	8	81
3	-395	1115	6.1	-	18	-
4	-105	1060	-	-	189	938

## 5. Conclusions

We have obtained new spectra of KUG 1031+398 around  $H\beta$  and  $H\alpha$ . We have found that the emission-line spectrum of this object can be modelled with four components: an extended H II region, two narrow emission regions of Seyfert 2-type and a relatively narrow “broad line” component, well fitted by a Lorentzian profile.

We disagree with Mason et al. on the analysis of the emission line profile of KUG 1031+398, in the sense that we find no evidence for the presence of an “intermediate” component in which the forbidden lines are almost, but not completely, suppressed by collisional de-excitation. Nevertheless, we find that this object is exceptional in having a “narrow” line region (defined as a region where  $\lambda 5007/H\beta \geq 5$ ) with almost the same width at half maximum as the “broad” line region (Balmer lines with no detectable associated forbidden lines); however, in the first case, the line-profile is Gaussian, while in the second case, it is Lorentzian.

*Acknowledgements.* We would like to thank A. Rodriguez-Ardila and G. Shields for useful comments and suggestions. A. C. Gonçalves acknowledges support from the *Fundação para a Ciência e a Tecnologia*, Portugal, during the course of this work (PRAXIS XXI/BD/5117/95 PhD. grant).

## References

Alloin D., Pellat D., Boksenberg A., Sargent W. L. W., 1983, ApJ 275, 493  
 Boller T., Brandt W. N., Fink H., 1996, A&A 305, 53  
 Boroson T. A., Green R. F., 1992, ApJS 80, 109  
 Breeveld A. A., Puchnarewicz E. M., 1998, MNRAS 295, 568

Brotherton M. S., Wills B. J., Francis P. J., Steidel C. J., 1994, ApJ 430, 495  
 Crenshaw D. M., Peterson B. M., 1986, PASP 98, 185  
 Espey B. R., Turnshek D. A., Lee L. et al., 1994, ApJ 434, 484  
 Ferguson J. W., Korista K. T., Baldwin J. A., Ferland G. J., 1997, ApJ 487, 122  
 Filippenko A. V., Sargent W. L. W., 1985, ApJS 57, 503  
 Greiner J., Danner R., Bade N. et al., 1996, A&A 310, 384  
 Lemaître G., Kohler D., Lacroix D., Meunier J.-P., Vin A., 1989, A&A 228, 546  
 Mason K. O., Hassall B. J. M., Bromage G. E. et al., 1995, MNRAS 274, 1194  
 Mason K. O., Puchnarewicz E. M., Jones L. R., 1996, MNRAS 283, L26  
 Massey P., Strobel K., Barnes J. V., Anderson E., 1988, ApJ 328, 315  
 Netzer H., Laor A., 1993, ApJ 404, L51  
 Oke J. B., 1974, ApJS 27, 21  
 Osterbrock D. E., 1974, *Astrophysics of gaseous nebulae*, Freeman and company, San Francisco  
 Osterbrock D. E., 1978, *Physica Scripta* 17, 285  
 Osterbrock D. E., 1987, *Lecture Notes in Physics* 307, 1  
 Pounds K. A., Allen D. J., Barber C., et al., 1993, MNRAS 260, 77  
 Pounds K. A., Done C., Osborne J. A., 1995, MNRAS 277, L5  
 Puchnarewicz E. M., Mason K. O., Cordova F. A. et al., 1992, MNRAS 256, 589  
 Puchnarewicz E. M., Mason K. O., Siemiginowska A., Pounds K. A., 1995, MNRAS 276, 20  
 Puchnarewicz E. M., Mason K. O., Siemiginowska A., 1998, MNRAS 293, L52  
 Pye J. P., McGale P. A., Allan D. J. et al., 1995, MNRAS 274, 1165  
 Rodriguez-Pascual P. M., Mas-Hesse J. M., Santos-Lléo M., 1997, A&A, 327, 72  
 Seaton M. J., 1975, MNRAS 170, 475  
 Shara M. M., Shara D. J., McLean B., 1993, PASP 105, 387  
 Shields G. A., 1978. In: Wolfe A.M. (ed.), *Pittsburgh conference on BL Lac objects*, University of Pittsburgh, Pittsburgh, Pennsylvania, p. 257  
 Stüwe J. A., Schulz H., Huehnermann H., 1992, A&A 261, 382  
 Takase B., Miyauchi-Isobe N., 1987, *Ann. Tokyo astron. Obs. 2nd series* 21, 363  
 van Groningen E., de Bruyn A. G., 1989, A&A 211, 293  
 Veilleux S., 1991, ApJ 369, 331  
 Wang T., Brinkmann W., Bergeron J., 1996, A&A 309, 81